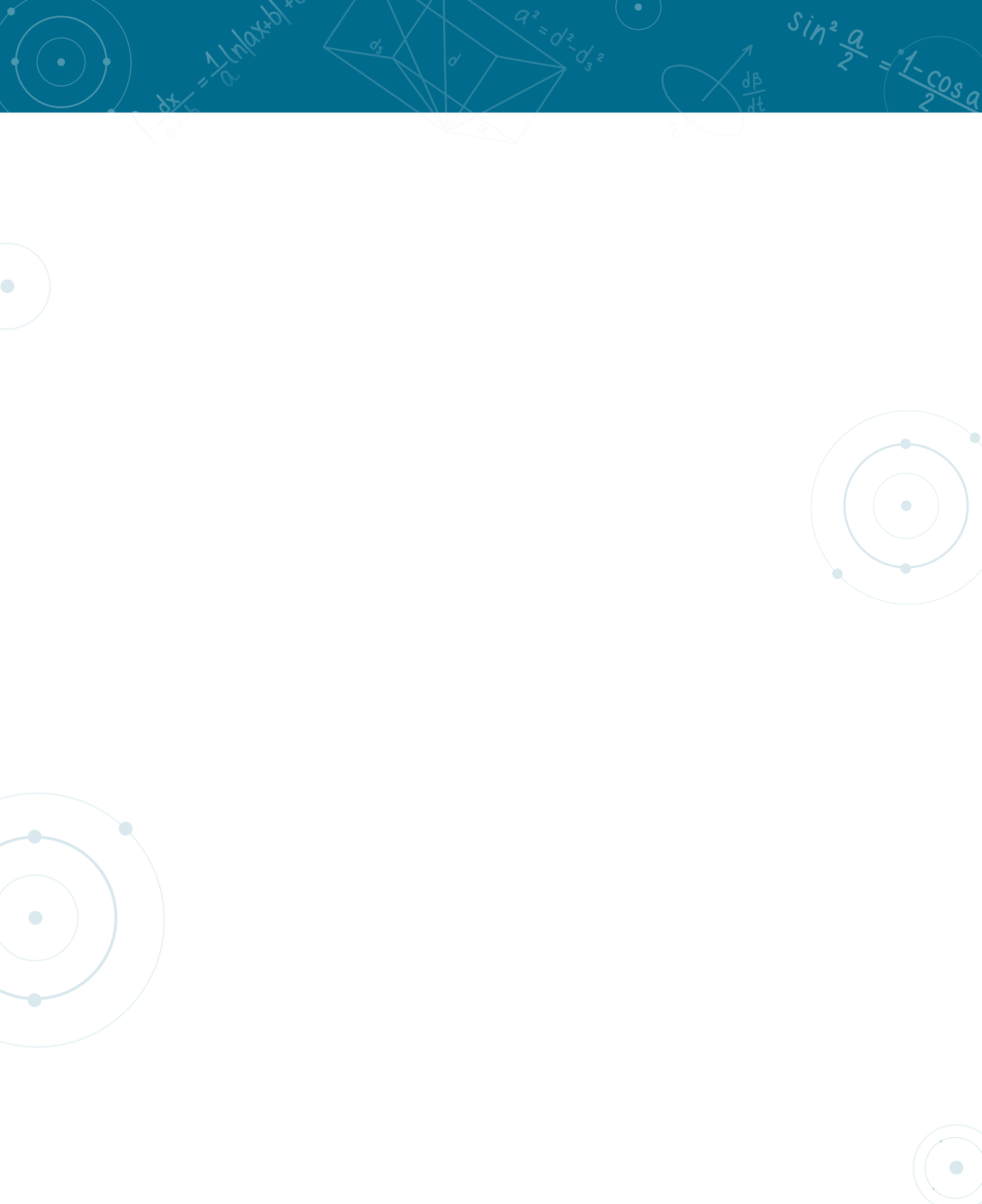


SCOR Paper

ACTUARIAL AWARD

Modeling the risk of frost in France

By **Laura Cohen** and
Dulcy Gninghaye
Winners of the French
Actuarial Award 2015
ENSAE ParisTech



Modeling the risk of frost in France

Laura Cohen et Dulcy Gninghayé
ENSAE ParisTech

Abstract

Key words: natural disaster, frost, catastrophe modeling, clustering, EOF, Generalized Linear Model, Peak Over Threshold, time series, copula, vulnerability curve, AEP, OEP.

Over the past few years, the economic impact of natural catastrophes on populations has clearly increased, jeopardizing the financial strength of insurance companies. Insurers thus need to measure the underlying risk and the losses their clients would experience from it. However, due to the unpredictability of natural disasters, specific catastrophe models must be designed in order to increase insurers' understanding of these risks and their consequences in terms of insurance.

This paper aims to design a catastrophe model for the risk of frost in France. Frost being directly linked to temperature, the first part consisted in reducing the dimension of the study by defining temperature-homogeneous regions, enabling to later model each of them as a whole. In the second part, frost was modeled from historical data, enabling the stochastic simulation of possible future events in France. After building custom vulnerability curves, we were able to deduce the economic losses triggered by the simulated events on AXA's portfolio. Finally, results associated with each event were put together to determine AXA's distribution of losses associated with frost events in France.

1. Introduction

With Solvency II set to go into effect soon, all insurers must have the best possible knowledge of all the risks they face. In this directive, specific treatment is called for with respect to natural disasters, whose impacts can be devastating for insurance companies. For example, Hurricane Andrew, which occurred in Florida in 1992, caused eleven insurers to go bankrupt.

When natural disasters are discussed, frost risk is rarely mentioned because its occurrence does not usually have as dramatic an impact as earthquakes, hurricanes, or volcanic eruptions. However, the duration of a frost event, as well as the high number of affected policies, can lead to heavy losses, as was the case for AXA in 2012, a particularly cold year. The purpose of this article is to build a catastrophe model for frost risk, allowing to simulate the occurrence of this risk and its related losses.

This modeling is done in four stages. First, we establish a clustering of the regions of France based on their temperatures, in order to reduce the amount of information available. Then, in the following two sections, we detail the construction of two modules of a catastrophe model, adapting them specifically to frost risk. The first module allows us to generate frost events in France over a year and the second module attempts to calculate the impact of these events on the AXA portfolio, translating physical events into economic losses. In the last section, we study the distribution of losses caused by frost that are obtained as outputs of the model.

2. Catastrophe modeling

Generally, in order to evaluate the distribution of losses related to a specific risk in non-life insurance, the frequency-cost approach is used. However, this approach is not applicable to disaster risks because the underlying assumption is that the distribution of past events is representative of that of future events. But natural disasters are by definition extreme and rare events, dependent on physical phenomena that cannot be modeled by this conventional statistical approach.

In order to more accurately estimate disaster risks, it is therefore necessary to use exposure-based approaches rather than historical ones. Catastrophe models combine the mathematical representation of the timing of claims with scientific characteristics of the insured risk to generate a distribution of losses.

Catastrophe models have become indispensable because they allow insurers to:

- Price reinsurance policies so as to optimize the risk transfer to reinsurance;
- Manage and diversify risks;
- Estimate the level of reserves needed to cover a loss;
- Minimize the Solvency 2 capital requirement;
- Anticipate natural disasters and predict losses to increase resilience.

A catastrophe model is structured into three independent modules: the Hazard Module, the Vulnerability Module and the Financial Module.

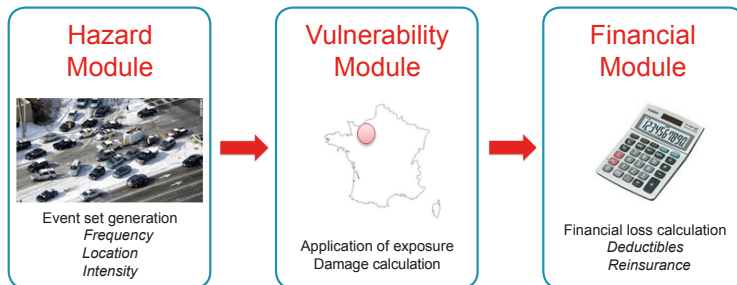


Figure 1 Structure of a catastrophe model

The **Hazard** Module, the central element in any catastrophe model, aims to replicate the physical phenomenon underlying the risk. In the case of frost risk, we seek to replicate physical phenomena related to temperature. This paper focuses mainly on the construction of this module, which includes the main challenges of catastrophe modeling.

The Hazard module having formed a significant dictionary of physical events, the **Vulnerability** module then quantifies the loss experience associated with each event through an estimate of the loss.

The **Finance** Module aims to determine the final losses of the insurer, net of insurance terms (the features of each policy purchased, the reinsurance terms, and the co-insurance share). For confidentiality reasons, this module will not be detailed here.

3. Clustering of regions

Frost being directly dependent on the observed temperature, different temperature scenarios must be simulated in order to deduce the occurrence of frost events. For this, we use historical data (23,193 days) of daily minimum temperatures recorded at 250 points located throughout France. But because modeling the temperature in each of these 250 points would be tedious, it is necessary to reduce the amount of information in space and time in order to obtain regions of France that are homogeneous in terms of temperature.

For this purpose, statistical methods of factor analysis of mixed data and/or classification are appropriate. In some cases, some authors recommend applying an explanatory factor analysis method and then a classification based on the results of the first method. This has the advantage of refining the information and results obtained.

We start by applying the Empirical Orthogonal Function (EOF) method, which resembles a Principal Component Analysis (PCA) but is more suitable for spatio-temporal data. Then, we conduct a classification method on the first principal coordinates obtained with the EOF method.

3.1. The Empirical Orthogonal Function (EOF)

The EOF method seeks to determine a new sample of variables to capture a significant part of the information observed on the data through a linear combination of the initial variables. It is widely used by meteorologists.

Applying the EOF method, we obtain a data array containing the 250 initial points and the 250 principal axes in columns. The main axes are obtained by linear combination of the initial temporal variables.

The first axis contains more information than the second, the second more than the third, and so on. Considering the decrease in information contained in each axis, it is necessary to focus the analysis on the first principal axes.

The following figure shows the eigenvalues scree and percentages of inertia associated with the first ten principal components.

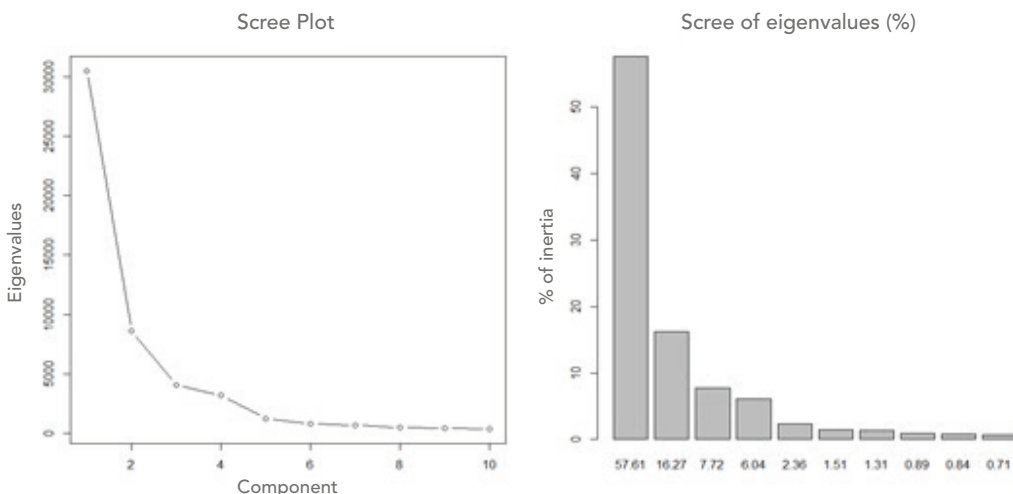


Figure 2 Eigenvalues scree

Looking at the first graph, the elbow rule means choosing the first 4 values. Using the second chart, we see that the inertia explained by the first 4 main areas is 87.63%.

To briefly describe the main trends associated with these four main areas, we represent for France the points with a significant contribution to the formation of each main axis considered. Figure 3 allows us to highlight different areas that are placed in opposition on the various axes.

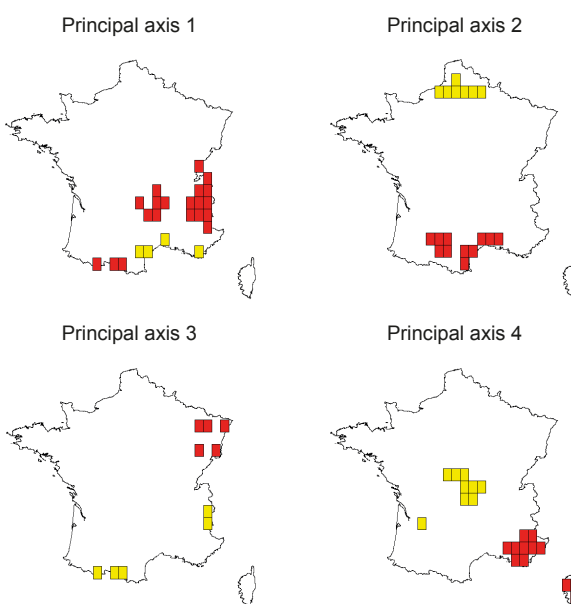


Figure 3 The geographic points best represented in the first 4 principal axes

On the first factorial axis, we note a contrast between the mountains (red points) and areas with a Mediterranean climate and mild winters (yellow points). The second factorial axis clearly highlights a contrast between Northern points with an oceanic climate and Southern points with a Mediterranean climate. On the third factorial axis, we see a contrast between regions with a climate under mountain influence (yellow points) and those whose climate instead shows a semi-continental influence (red points). The fourth and last factorial axis highlights the contrast between the areas with a Mediterranean climate, including Corsica and the French Riviera (red points), and the Massif Central (yellow points).

3.2. The clustering

After applying the EOF method, we obtain a matrix representing our 250 geographic locations on the first 4 major axes used. An Ascending Hierarchical Clustering (AHC) is then applied to these points using Ward's criterion.

The dendrogram derived from the AHC is presented below:

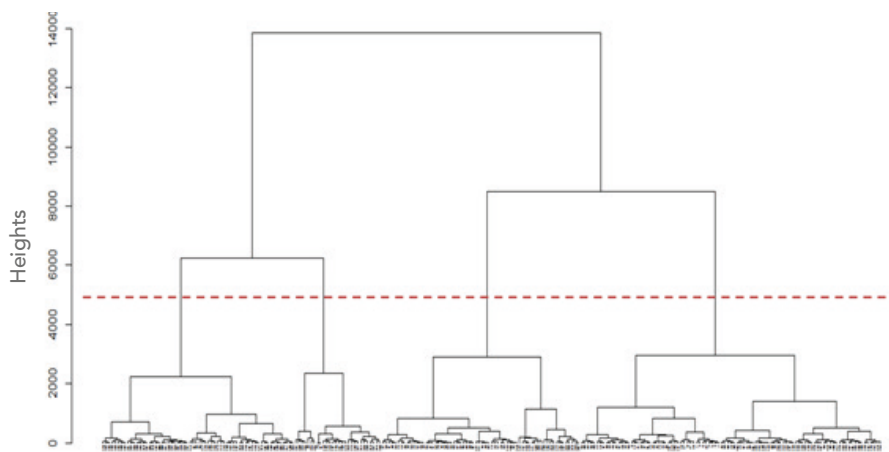


Figure 4 Dendrogram associated with the AHC (Ascending Hierarchical Clustering) on the coordinates of the first 4 principal axes of the EOF

Depending on the level where the dendrogram is «cut,» classes are obtained. Based on the principle of parsimony, we want to end up with the smallest number of classes possible.

To ensure homogeneity of temperatures within each region, we cap the standard deviation of their respective temperatures at 2° Celsius.

These different criteria lead us to select four classes shown below.



Figure 5 Segmentation of France into 4 regions (results of ACH following the EOF)

The first class, which is green, includes part of Southern France. It is characterized by cities with a temperate climate and mild winters. The area in Southwest France is characterized by a temperate oceanic climate and includes cities such as Bordeaux and Limoges. The rest of the geographic locations in this first area are characterized by a Mediterranean climate and include cities such as Nice, Marseille, Perpignan, and Toulon, as well all of Corsica.

The second class, in red, covers Northwest France and comprises areas influenced by an oceanic climate. It includes cities such as Paris, Lille, Caen, and Rennes.

The third class, in purple, includes Northeast France and parts of Central France. This area is under the influence of a semi-continental climate and contains regions of average altitude. It includes cities like Strasbourg, Nancy, and Dijon. It also includes a point in Southeast France, a mid-altitude region near the Pyrenees.

The fourth class, in cyan blue, features a sub-alpine influence and includes cities such as Saint-Etienne and Grenoble.

4. Construction of the Hazard module

The Hazard module aims to stimulate several frost scenarios in France. The clustering completed in the previous section has made it possible to reduce the scale of the problem to just four points in order to simulate frost scenarios in each region.

The construction of the hazard module is a three-step process:

- the characterization of a frost event, highly dependent on temperatures;
- the statistical modeling of the regional temperature, taking inter-regional correlations into account;
- the simulation of several temperature scenarios in order to deduce frost events.

4.1. Characterizing a frost event

Physically, frost is due to freezing temperatures. However, the occurrence of freezing temperatures does not necessarily generate losses for the insurer. What interests us is an insurance-covered frost event, i.e., a frost event that causes losses for insurers. This complicates the characterization of the phenomenon. It is intuitive to assume that the occurrence of a frost event covered under an insurance policy is also related to temperature, but we have to wonder how temperature affects this phenomenon. For example, is frost occurrence related to the temperature on the day the loss occurs or rather to temperature changes observed over time? And for how many losses?

Characterizing frost is thus a process that occurs in two phases, including:

- the search for variables that explain the occurrence of the frost;
- the modeling of historical losses that are connected to the explanatory variables previously found.

In the first phase, we take as the target variable to be explained the occurrence or non-occurrence of frost. The occurrence of a frost event is materialized by the filing of a claim. We use as explanatory variables the daily minimum temperatures in each geographic location as well as temperature variations over different periods. Using logistic regressions, we test various combinations of these variables. We finally settle on the temperature differences over 20 days, the daily minimum temperature and the region.

In the second phase, the determinants previously highlighted are used to model the daily frequency of losses given by:

$$\text{frequency} = \frac{\text{Number of daily losses}}{\text{Exposure}}$$

The exposition being known, this amounts to modeling the number of daily losses. In the traditional approach of modeling count variables, Poisson or negative binomial regressions are used.

The Poisson regression adapted for rare phenomena does not allow us to take into account the over-dispersion of the number of claims/losses in our study. The negative binomial regression, adjusted in the event of over-dispersion, underestimates the small number of claims (including zero losses for the days when there was no claim reported). Indeed, the negative binomial regression is not very effective given the significant variations in magnitude of the number of reported claims (minimum 0, maximum 700, standard deviation 50 claims). In addition, the data contain a large number of zeros. Indeed, out of the 1,646 observations contained in the data table, 716 do not experience any loss.

Given the large number of zeros, we turn to the counting models with excess zeros: zero inflated and hurdle. Based on our analyses, the hurdle model was chosen. After a backtesting of the model simulating the number of claims through a hurdle regression, it is clear that this model underestimates the number of claims for all years. Indeed, the estimated total loss for all years is equal to 81% of historic total claims between 2008 and 2012. By looking at each year in detail, we realize that the year 2012, which alone contains nearly 76% of the total number of claims, is widely underestimated in the model, with a prediction deviation of -72%. The hurdle model has a hard time addressing these extremes. It actually smoothed the observations, sharply overestimating the years where there were few claims and underestimating those where there were many claims. But our goal is precisely to capture extreme events in a catastrophe model. So this model is not suitable for the study.

The extremely cold temperatures and the number of large claims in 2012 observed lead us to believe that the claims are triggered massively as soon as a given temperature threshold is reached.

To determine this temperature threshold, we use the mean excess function. In theory, the extreme temperature threshold is one from which temperatures can be modeled by a generalized Pareto law. In practice, the threshold chosen must be a breaking point in the shape of the mean excess function.

Figure 6 shows the plot of the mean excess function for the regional average temperature (tminMoy). To facilitate graph reading of the mean excess function, we have plotted $-tminMoy$.

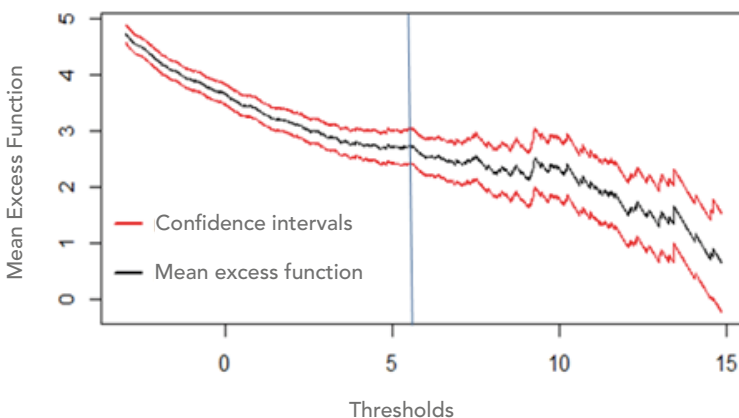


Figure 6 Mean Excess function of tminMoy

Therefore, we set our threshold at -5.5°C , allowing us to split our data into two subpopulations:

- the observations for which $-5.5^{\circ} < \text{tminMoy} < 3^{\circ}$, i.e., 1,352 observations;
- the observations for which $\text{tminMoy} \leq -5.5^{\circ}$, i.e., 294 observations.

For each subpopulation, we search for the model that best adjusts the number of claims.

For the first sample, due to the over-dispersion of the number of claims and excess zeros in the data, the hurdle model is best suited.

For the second sample, conventional counting models are best suited, because the problem of excess zeros in the database has disappeared. On the other hand, the data is still over-dispersed. Thus negative binomial regression turns out to be the most appropriate.

4.2. Modeling the temperature

As frost is directly dependent on the temperatures observed, and more particularly on the magnitude of temperature shifts, it is necessary to model the temperature in France in order to be able to deduce the occurrence of frost events. This modeling is performed on the average daily temperatures (since 1950) in the four regions of the classification.

The Box & Jenkins approach (1976) is used. The initial temperature series (X_t) breaks down as follows:

$$X_t = m_t + s_t + Y_t$$

With:

- m_t : trend
- s_t : seasonality
- Y_t : the residual series

Initially, we try to adjust an ARMA model to Y_t . An ARMA model (p,q) can be broken down into two processes: an AR (Auto Regressive) process of order p and an MA (Moving Average) process of order q . So (X_t) an ARMA(p,q) process, verifying the following equation:

$$X_t = \sum_{i=1}^p \varphi_i X_{t-i} + \sum_{i=1}^q \theta_i \varepsilon_{t-i} + \varepsilon_t$$

The term ε_t is commonly referred to as residual. To validate this model, ε_t must be a Gaussian white noise:

- ➊ The residuals must be stationary, i.e., the variance must be constant over time;
- ➋ The residuals must be independent;
- ➌ The residuals must be Gaussian.

To ensure that the residuals are stationary, we use a graphic criterion. So in Figure 7, we draw a box plot summarizing some features of the series studied (median, quartiles, minimum, maximum, and deciles). For this purpose, the values taken by ε_t are regrouped by month. There is an observed dispersion of the values of this process by month: ε_t values are more dispersed during the winter months than during the summer months, which proves that ε_t is not white noise. The ARMA model is thus ruled out.

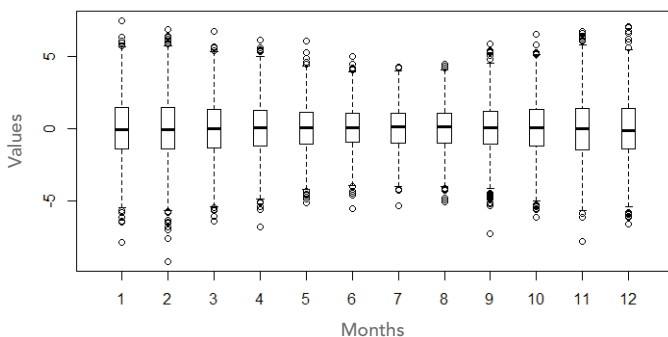


Figure 7 Residuals dispersion by month

This dispersion must be taken into account in the rest of the study to obtain a suitable model. Moreover, the dispersion appears seasonal, as it is obviously higher during the winter months. Accordingly, we test a periodic variance linear model to account for the seasonality of residuals.

The initial series thus breaks down as follows:

$$X_t = m_t + s_t + p_t + Y_t$$

With:

- ➊ s_t : seasonality
- ➋ m_t : trend
- ➌ Y_t : an ARMA process to estimate with $\text{Var}(Y_t) = 1$. In the preceding section, $\text{Var}(Y_t)$ was not constant
- ➍ p_t : l'écart type de la série, supposé périodique de périodicité annuelle.

For this periodic variance model, all assumptions (stationary, independent, and Gaussian residues) are verified in each region. Thus, this model is selected for the subsequent study.

4.3. Modeling inter-region dependency

This part aims to stimulate different temperature scenarios from the four previously modeled series. Since temperature is a homogeneous phenomenon, simulation in the four regions cannot be done independently. In fact, if a temperature spike is observed in one region of France, it is very likely that other regions are also affected by this spike.

To reflect this geographic dependency, we use the copula theory to characterize the dependency among several random variables. We want to determine the parametric copula best suited to our data and that best reflects the dependency relationships between residuals. There are two main parametric copula families: the elliptical copulas and Archimedean copulas. The search for the optimal copula is performed on a set of four parametric copulas selected a priori: (i) Gaussian and Student (elliptical copula) and (ii) Gumbel and Clayton (Archimedean copulas).

Using the CML (Canonical Maximum Likelihood) estimation procedure, we find – for each of the four parametric copulas selected – the corresponding parameters maximizing the likelihood. The objective now is to compare the results obtained using these four copulas with empirical residual data. We will select the parametric copula that best models the dependency structure of residuals.

Initially, we use the dependogram that represents the dependence structure in the form of a point cloud of simulations of a theoretical copula. We compare the dependogram of the empirical copula with that of the four parametric copulas selected. The dependogram allows us, in addition, to observe the more or less simultaneous nature of the productions from the sample. In the tails, more specifically, it will be useful to analyze whether simultaneity is high and therefore if it is necessary to calibrate in our sample a copula with tail dependence.

In Figure 8, we have represented the dependograms associated with the empirical copula and the parametric copulas for the residues that correspond to Region 1 (Southern Region) and Region 2 (Northwest Region) for 20,000 simulations. The results are similar for the other five couples.

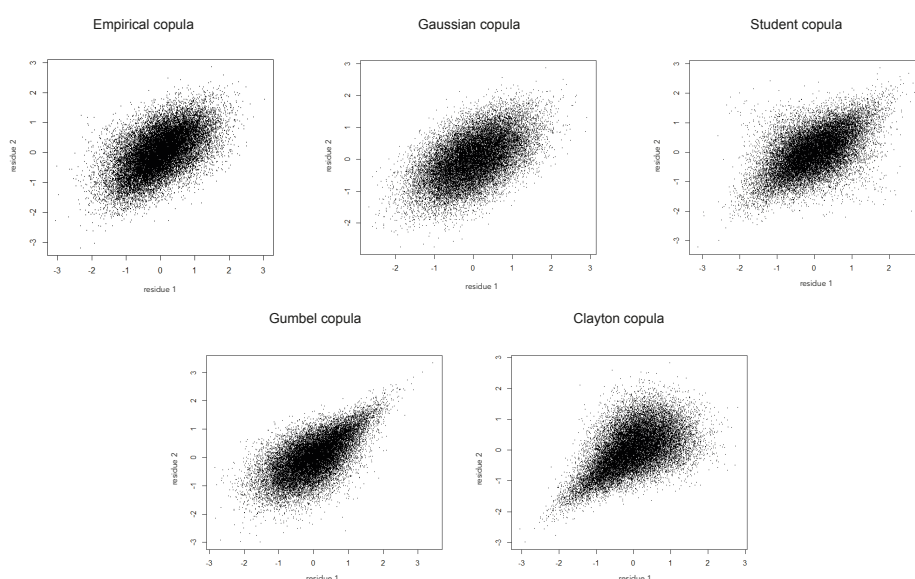


Figure 8 Dependograms associated with the empirical copulas and parametric copulas for residuals 1 and 2

Compared to other copulas, the Student and Gaussian copulas seem to fit the true underlying dependency structure of the data represented by the empirical copula. We can also note that the Student copulas can better model the dependency of extreme points and thus seems better suited for the empirical data. The AIC and BIC criteria, taking into account the number of parameters, confirm the choice of the Student copula. Although it has the largest number of parameters, the likelihood of the model is large enough not to be penalized by the high number of parameters.

4.4. Scenario simulations

The aim of this section is to regroup all of the preceding results to construct frost scenarios over a period of one year in France. To this end, we start by simulating several temperature scenarios over one year in order to then deduce frost events.

Temperature scenarios

We use the modeling of regional temperatures and the copula theory to jointly simulate the residuals associated with each region. Then we simulate 10,000 temperature scenarios for the following year. Our temperature data stop on July 1, 2013, so we are building 10,000 temperature scenarios from July 2, 2013 to July 2, 2014 for each of the four regions. The simulated temperatures are the average minimum temperatures in each region.

Figure 9 represents the predicted temperatures in each region for the first scenario. The black curve represents the temperatures observed since August 2011, while the red curve represents a temperature scenario for the following year.

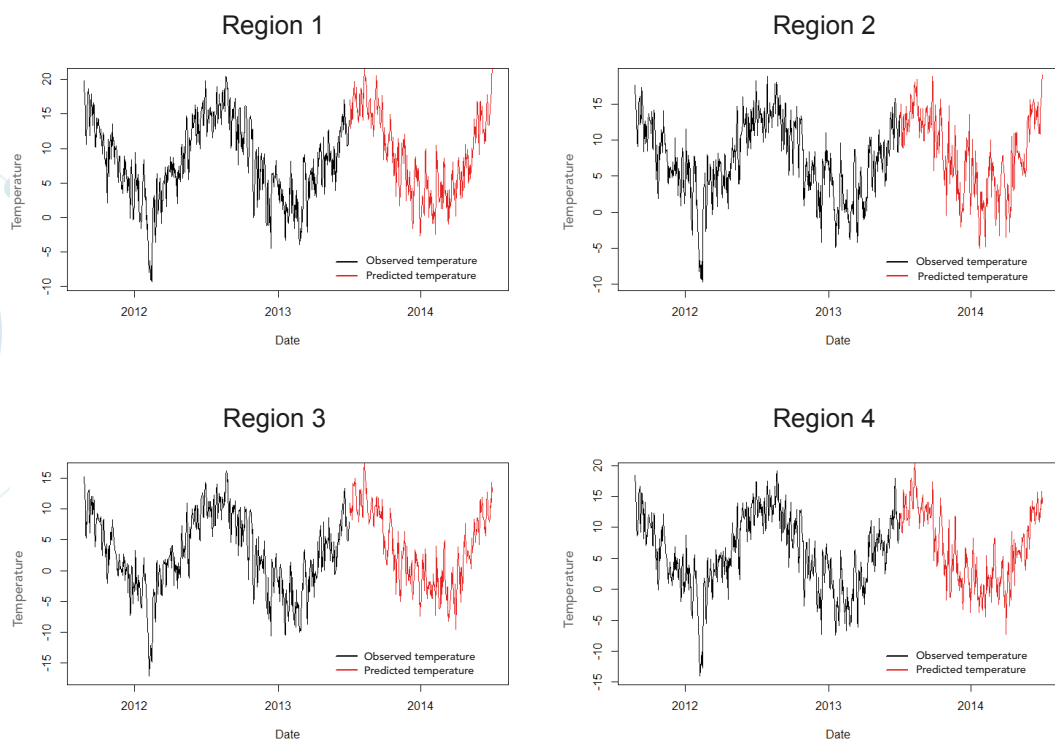


Figure 9 Sample temperature scenario by region, from July 2013 to July 2014

Figure 10 represents the temperatures simulated in the four regions. This graph illustrates the clear correlation between regions that was obtained by using the copula.

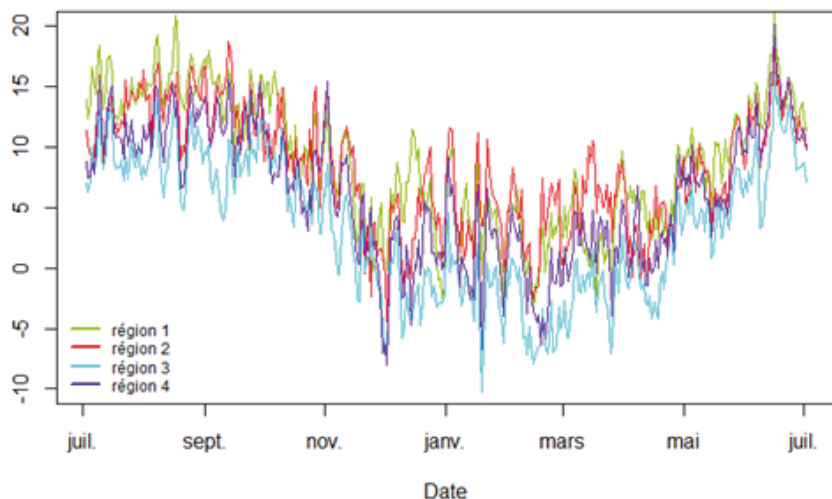


Figure10 Sample of a temperature scenario in the four regions

The minimum and maximum temperatures for all the scenarios are, respectively, -30° C and 34° C . These two values are more extreme than the historical values (respectively, -19° C and 23° C). This seems consistent, nevertheless, as 10,000 scenarios / years were simulated and we have a record spanning 63 years. It should be noted that the observed minimum temperature in France since 1947 was -32° C .

Event scenarios

The temperatures having been simulated, we have the average minimum temperature in each region. From this information, we deduce the temperature differences over 20 days. It is then a question of predicting claim counts in each region, factoring in the threshold of -5.5° C on the day of the incident and the season. Indeed, the prediction should be performed only during the winter and when the temperature is less than 3° C . When this temperature is strictly greater than -5.5° C , the claim predictions use the hurdle regression. Otherwise, the prediction uses negative binomial regression. In the remaining cases, in summer or when the temperature is above 3° C , we predict the number of claims to be zero.

We also assume that exposure by region is consistent from year to year. Finally, we get 10,000 scenarios giving the daily loss probability for a given policy within each region during an annual period.

5. Construction of the Vulnerability module

In this section, our aim is to model the loss associated with various pieces of insured property when a frost event occurs. This module provides destruction curves (or vulnerability curves) that model the distribution function of destruction rates¹ observed during a frost event. In a conventional catastrophe

¹Amount of the loss divided by the value of the insured property

model, the curves combine destruction rates depending on the intensity of the event considered. For frost risk, we consider that losses caused by frost do not depend on the intensity of the event. Indeed, when it occurs, a frost event usually causes very similar losses regardless of the trigger threshold. So here, we assume that the claim declared when a frost event occurs only depends on the type and value of the property insured and not on the intensity of the event, which is reflected in the probability of loss in the Hazard module.

To model the vulnerability of assets to frost, we calibrate curves of the parametric family MBBEFD (Maxwell-Boltzmann, Bose-Einstein, Fermi-Dirac). This method was popularized by an article by S. Bernegger² and has become a standard in the insurance industry for several reasons:

- The MBBEFD curves are used to model the probability of destruction of property by taking the discontinuities into account. For example, some properties can undergo destruction that is either minor or total and the distribution of the destruction rate function therefore presents discontinuities.
- These can take very diverse shapes: convex, concave, inflection points, etc.

There are two ways to define a MBBEFD curve. The general method requires two parameters. There is also a special case of the general method, called Hyperbolic MBBEFD, which requires a single parameter. The MBBEFD method has a parameter used to calibrate destruction curves more easily while also delivering more robust results. For this reason, we choose to adopt this method in the study. In addition, this is the most widely used method in practice.

The first method thus allows us to define the density function associated with the destruction rate of property by:

$$f(x) = \frac{1}{m \cdot \left(1 + \frac{x}{m}\right)^2} \cdot \mathbf{1}_{0 \leq x < 1} + p \cdot \mathbf{1}_{x=1}$$

This function only depends on the m parameter, which is the median destruction rate associated with the property. For each type of property, we are able to calculate the m parameter associated with linear regressions on AXA's loss experience between 2008 and 2012.

As an example, we draw the destruction curves related to five insured sum values for the home insurance LoB.

²"Swiss RE exposure curves and the MBBEFD distribution class", 1997



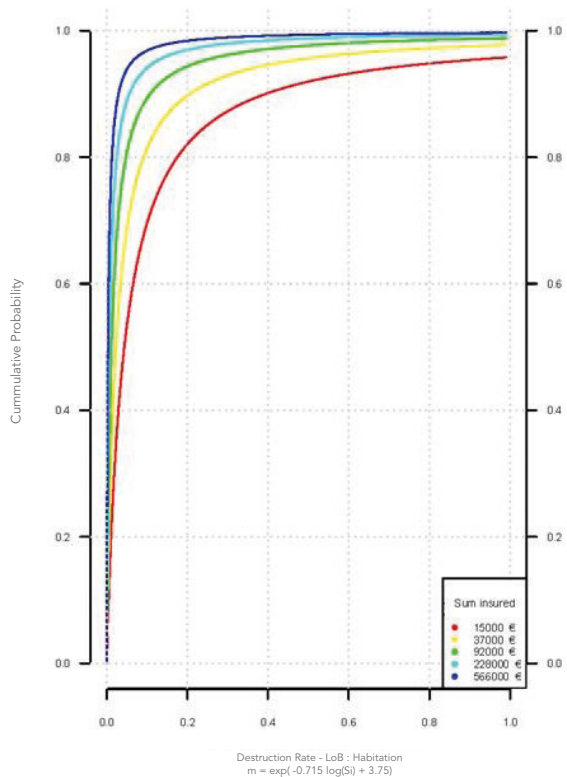


Figure 11 Destruction curves for the Home Insurance LoB

6. Results of the model

The principal results of a catastrophe model are synthesized by the AEP and OEP curves:

- **The OEP curve** (Occurrence Exceedance Probability): associates a return period³ (in years) to the maximal loss generated by an event over one year. The OEP thus characterizes the annual probability that a single event produces losses in excess of a certain amount.
- **The AEP curve** (Aggregate Exceedance Probability): associates a return period (in years) to the total loss generated by the full set of events over one year. The AEP thus characterizes the annual probability that the full set of events over one year generates losses in excess of a certain amount. So an AEP curve is always higher than an OEP curve.

³A return period corresponds to the inverse of the statistical frequency of an event among a set of events (annual) that are equally likely. It must therefore be interpreted as a statistical probability. It is expressed in years and corresponds to the probability of a scenario occurring. For example, an event with a 200-year return period has a 0.5% probability of occurring in one year.

These curves are used to set regulatory capital requirements under Solvency II and the optimal reinsurance coverage to purchase.

The AEP and OEP curves of our model are obtained by coupling the Hazard, Vulnerability, and Finance modules. For reasons of confidentiality, the Finance module which allows to take into account the characteristics of the policies written and the reinsurance conditions, will not be detailed here. We thus are considering here the gross loss before the application of financial conditions.

The daily frost events generated for each region with the Hazard module, must be applied to the portfolio to translate the probability of occurrence in a financial loss. To this end, the policies in the AXA France portfolio are grouped according to their geographic location within one of the 4 regions of our segmentation. For each day of each annual regional scenario, we first assess the loss caused by frost on every policy, then we add them up to derive the total loss for the AXA portfolio for each scenario.

Figure 12 shows the AEP and OEP curves for return periods from 1 to 250 years. For privacy reasons, the loss amounts are not disclosed. However, the x value associated with the y-axis represents the total gross loss of AXA caused by frost during the year 2012. Therefore, we can determine that the return period associated with this event on the AEP curve is eight years.

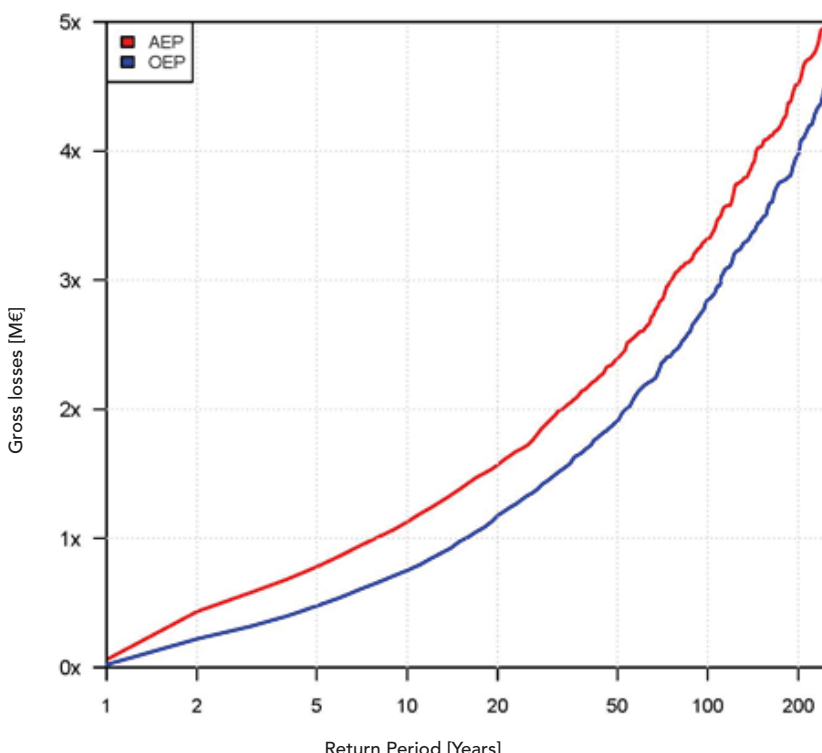


Figure 12 AEP and OEP curves

Conclusion

The objective of this paper was to build a catastrophe model for frost risk. A catastrophe model combines three modules, each one providing specific information. This paper focused on the construction of the first two: the Hazard module and the Vulnerability module. The Finance module is produced in-house at AXA for confidentiality reasons. At the end of the study, we got a distribution of gross losses resulting from the application of frost risk modeling to the exposed AXA France portfolio.

Unlike conventional catastrophe models, where events are simulated in a one-off and thus not consecutively, the approach adopted here allows us to provide daily information on the occurrence of claims related to frost. This information is undoubtedly valuable for an insurer, both in terms of reinsurance optimization and frost risk management.

This approach also has the advantage of being flexible and adaptable. The model has been designed so as to integrate new countries while also taking their correlation into account. Since the results for France appear credible and consistent with AXA's historical losses, this model has since been extended to other European countries.

Lastly, the model could be adapted to construct another major climate risk: the risk of drought. Drawing on the methodology of this study, it would have to consider the maximum temperatures and type of soil, however.

Bibliography

- BERNEGGER S., 1997, The Swiss RE exposure curves and the MBBEDF distribution class
- BJÖNRSSON H. & VENEGAS S.A., 1997, A manual for EOF and SVD – Analyses of Climatic Data, McGill University
- CAMERON, A.C. & TRIVEDI, P.K., 1998, Regression analysis of count data, Cambridge, Cambridge University Press
- CAMERON, A.C. & TRIVEDI, P.K., 2005, Microeconometrics: Methods and Applications, Cambridge, Cambridge University Press.
- CASIEZ G., Dynamic Time Warping : déformation temporelle dynamique, Université de Lille
- CHARPENTIER A., DUTANG C., L'Actuariat avec R
- CHAVEZ-DEMOULIN V. & DAVISON A.C., 2012, Modelling time series extremes, Volume 10, Number 1, P 109–133
- CREPON B. & JACQUEMET N., 2010, Econométrie : méthodes et applications, De Boeck
- DENUIT M. & CHARPENTIER A., 2005, Mathématiques de l'assurance non-vie, Tome II, Economica
- EUROPEAN CLIMATE ASSESSMENT & DATASET, <http://eca.knmi.nl/>
- FERMANIAN, J.D., 2014, Théorie des copules, support de cours ENSAE
- FFSA, 2012, Rapport annuel
- FLYNN M. & FRANCIS L. A., 2009, More flexible GLMs zero-inflated models and hybrid models, Casualty Actuarial Society E-forum
- GORGÉ G., 2013, Insurance Risk Management and Reinsurance
- HANNACHI A., 2004, A Primer for EOF Analysis of Climate Data, Department of Meteorology, University of Reading U.K
- HUGUES G., RAO S. & RAOT, 2006, Statistical analysis and time-series models for minimum/maximum temperatures in the Antarctic Peninsula
- KHAROUBI-RAKOTOMALALA C. 2008, "Les fonctions copules en finance", Université de la Sorbonne
- LEDOLTER J., 2013, Datamining and business analytics with R, Wiley
- LOPEZ O., 2014, Econométrie de l'assurance, support de cours ENSAE
- ROBERT Y. C., Théorie des Valeurs Extrêmes, support de cours ENSAE
- RONCALLI T., 2002, Gestion des risques multiples ou copules et aspects multidimensionnels du risque, support de cours ENSAI
- RONCALLI T., FRACHOT A., 2009, La Gestion des Risques Financiers, Economica
- ROUSTANT O., 2003, Produits dérivés climatiques : aspects économétriques et financiers
- SAKOE H., CHIBA S., 1978, Dynamic programming algorithm optimization for spoken word recognition
- SAPORTA G., 2011, Probabilités, Analyse de données et Statistique, Technip
- SKLAR A., 1959, Fonctions de répartition à n dimensions et leurs marges, Publications de l'Institut de Statistique de l'Université de Paris
- STRAUSS D., 2009, Empirical Orthogonal FunctionAnalysis (Principal Component Analysis), ICTP
- SWISS RE, 2003, Catastrophes naturelles et réassurance
- SWISS RE, 2003, Introduction à la réassurance
- ZEILEIS A., KLEIBER C. & JACKMAN S., 2008, Regression models for count data in R, Journal of statistical software, Volume 27, Issue 8

SCOR Paper N°27 - October 2013	Are great earthquakes clustered?
SCOR Paper N°28 - February 2014	Solar storms and their impacts on power grids - Recommendations for (re)insurers
SCOR Paper N°29 - September 2014	A game-theoretic approach to non-life insurance market cycles
SCOR Paper N°30 - September 2014	Explicit Föllmer-Schweizer decomposition of life insurance liabilities through Malliavin calculus
SCOR Paper N°31 - January 2015	The use of economic scenarios generators in unstable economic periods
SCOR Paper N°32 - March 2015	An Integrated Notional Defined Contribution (NDC) Pension Scheme with Retirement and Permanent Disability
SCOR Paper N°33 - April 2015	Exploring the Dependence between Mortality and Market Risks
SCOR Paper N°34 - November 2015	A Change of Paradigm for the Insurance Industry
SCOR Paper N°35 - January 2016	The Globalization of Infectious Diseases
SCOR Paper N°36 - February 2016	Spatial Risk Measures and Applications to Max-Stable Processes
SCOR Paper N°37 - March 2016	ALM Model: The contribution of Fuzzy Logic to behaviour modelling
SCOR Paper N°38 - April 2016	Explicit diversification benefit for dependent risks
SCOR Paper N°39 - December 2016	A General Framework for Modeling Mortality to Better Estimate its Relationship to Interest Rate and Risks
SCOR Paper N°40 - Juin 2017	On the Diversification Benefit of Reinsurance Portfolios

Each year, SCOR rewards the best academic work in the field of actuarial science with prizes in several countries throughout the world. These prizes, several of which are financed by the SCOR Foundation for Science, are designed to promote actuarial science, to develop and encourage research in this field, and to contribute to the improvement of risk knowledge and management. SCOR publishes a selection of the awarded papers in its SCOR Paper collection.